HHS Public Access

Author manuscript

Curr Opin Neurobiol. Author manuscript; available in PMC 2019 June 01.

Published in final edited form as:

Curr Opin Neurobiol. 2018 June ; 50: 179–189. doi:10.1016/j.conb.2018.03.008.

Towards circuit optogenetics

I-Wen Chen[1], **Eirini Papagiakoumou**[1,2], and **Valentina Emiliani**[1]

[1]Wavefront-Engineering Microscopy group, Neurophotonics Laboratory, CNRS UMR8250, Paris Descartes University, 45 rue des Saints-Pères, Paris, France

[2]Institut National de la Santé et de la Recherche Médicale (INSERM)

Abstract

Optogenetics neuronal targeting combined with single-photon wide-field illumination has already proved its enormous potential in neuroscience, enabling the optical control of entire neuronal networks and disentangling their role in the control of specific behaviors. However, establishing how a single or a sub-set of neurons controls a specific behavior, or how functionally identical neurons are connected in a particular task, or yet how behaviors can be modified in real-time by the complex wiring diagram of neuronal connections requires more sophisticated approaches enabling to drive neuronal circuits activity with single-cell precision and millisecond temporal resolution. This has motivated on one side the development of flexible optical methods for two-photon (2P) optogenetic activation using either, or a hybrid of two approaches: scanning and parallel illumination. On the other side, it has stimulated the engineering of new opsins with modified spectral characteristics, channel kinetics and spatial distribution of expression, offering the necessary flexibility of choosing the appropriate opsin for each application. The need for optical manipulation of multiple targets with millisecond temporal resolution has imposed 3D parallel holographic illumination as the technique of choice for optical control of neuronal circuits organized in 3D. Today 3D parallel illumination exists in different complementary variants, which privilege either simplicity or temporal precision or axial resolution. In parallel, the possibility to reach hundreds of targets in 3D volumes has prompted the development of low-repetition rate amplified laser sources enabling higher peak power, while keeping low average power for stimulating each cell.

All together those progresses open the way for a precise optical manipulation of neuronal circuits with unprecedented precision and flexibility.

Graphical abstract

Corresponding author: Valentina Emiliani (valentina.emiliani@parisdescartes.fr).

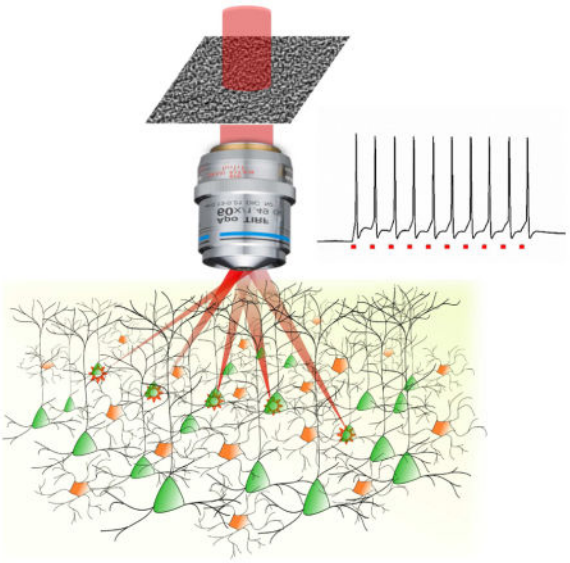

Introduction

Since the discovery of Channelrhodopsin[1] and the first demonstration of photo-evoked action potentials in mammalian cells[2], optogenetics is progressively revolutionizing neuroscience research, opening perspectives both in fundamental and in medical research still unimaginable until few years ago[3].

Joint progress in light delivering approaches, multi-photon laser sources development, and opsins engineering has now brought the field of optogenetics into a new phase that we can name “circuit optogenetics”, where neural circuits distributed between different brain areas can be optically interrogated and controlled with millisecond temporal precision and single-cell resolution. The circuit mechanisms underlying brain functions such as perception and behaviors can finally be revealed by linking the gradual changes in task performance with precise reproduction or modulation of the temporal sequences of neuronal excitability in a spatially specific ensemble.

Here, we review the main achievements in each of this field and anticipate the future needs that will make it possible to enlarge even more the use of optogenetics for brain circuits manipulation.

Light delivering approaches

Scanning and parallel illumination

As first demonstrated in 2009, efficient two-photon (2P) optogenetic control of neuronal activity can be achieved by raster or spiral scanning of a focused spot over the cell soma[4]. By continuously scanning along a spiral trajectory the cell soma for ≈ 30 ms, 2P action potential (AP) generation was first demonstrated in cultured neurons expressing Channerhodospin-2 (ChR2). The successive development of the slower opsin C1V1[5],

enabled to extend this approach to the photostimulation of neurons in acute brain slices and *in vivo* with total illumination duration ranging from 1 to 70 ms[6–9].

Alternatively to scanning activation, using scan-less light shaping approaches, such as low-numerical aperture (NA) Gaussian beams, Computer-Generated Holography (CGH)[10] (Figure 1a) or the Generalized Phase Contrast (GPC) method[11] (Figure 1b), enables to simultaneously illuminate the entire cell surface at once, thus minimizing the total illumination time for inducing an AP.

For patterned illumination, the quadratic (for low-NA Gaussian beams and GPC) or linear (for CGH) dependence of the axial extension on the lateral spot size[12,13] quickly deteriorates the axial resolution. As first demonstrated in 2008[13], when using 2P excitation this can be remedied by combining parallel illumination approaches with the technique of temporal focusing (TF)[14,15] (Figure 1c). After its first demonstration with plane-wave illumination in 2005 for imaging applications[14], TF was combined in 2008 with phase modulation of laser beams[13,16] and soon afterwards used for optogenetic activation: combined either with phase modulation techniques, GPC[17] and CGH[18], or low-NA beams[19–22], it has been possible to demonstrate efficient AP generation in cultured neurons and neurons in brain slices, using ChR2[17,19,22] and C1V1[18,20] by using 1 to 10-ms illumination duration. Patterned illumination with GPC and TF also enabled for the first time the simultaneous activation of multiple cells and multiple cell processes[17]. Notably, because TF reduces the instantaneously illuminated region to a line, it decreases the probability that non ballistic photons interfere with the ballistic ones in the tissue, thus enabling to preserve the illumination shape after several micrometres propagation through scattering media[18,23,24].

Multi-cell targeting

Parallel approaches present the great advantage of minimizing the illumination time with respect to their scanning counterparts. This can be seen as follows: the total illumination time for scanning activation, $T_{I.scan}$, roughly equals the illumination time per spot (t_{dwell}) multiplied by the number of scanned positions and by the number of targets, while that for parallel approaches, $T_{I.paral}$, is only given by t_{dwell}. As a consequence, for volumetric multi-cell targeting, $T_{I.scan}$ can largely exceed the value of $T_{I.paral}$ and three-dimensional (3D) parallel illumination remains the only option to achieve multi-target activation with millisecond temporal resolution[25].

As originally demonstrated for multi-trap optical tweezers, CGH can generate 3D multi-foci using ‘prisms and lenses’ algorithms[26]. Similar algorithms combined with visible or IR light have been successively used for 3D neuronal stimulation using 1P or 2P uncaging[27–30]. Optogenetic activation needs, however, illumination of membrane areas greater than the micrometric size of spots typically adopted for uncaging. A possible solution, originally proposed in Packer et al.[7], consists in generating in parallel multiple diffraction-limited spots via CGH at the positions of the targeted cells, and scanning the spots simultaneously over the cell membranes using a galvanometric-mirror-based system. Yet, the need of scanning over the cell body limited the achievable temporal resolution (illumination time for AP generation ≥11 ms; latency ≥20 ms; jitter ≥6 ms)[7,8]. Lately, the use of high-peak-power amplified excitation laser sources enabled to reduce both latency (<10 ms) and jitter (~1 ms)

using illumination durations of 10 ms and ~4.5 mW of average illumination power per cell. Shorter Illumination durations (1 ms) could be used to excite neurons, however this required 2 to 5 times more power per cell (~10–20 mW)[9]. Because efficient current integration under scanning photoactivation requires slow opsins, this approach limits the maximum achievable spiking rate. Moreover, the need for using focused light at saturation power to compensate for the small spot surface generates important out-of-focus excitation[4].

Alternatively, multi-target stimulation can be achieved by scan-less 3D generation of extended patterns using a 3D extension of the Gerchberg-Saxton[31] algorithm as proposed years ago in combination with low-NA objectives[32,33]. More recently, after being adapted to high-NA objectives and being incorporated with intensity compensation protocols[34], 3D-CGH was used to generate shaped patterns with uniform light distribution within an excitation field of 240×240×260 μm^3. With this approach, it was possible to drive tail bending by selective photoactivation of specific ensemble of premotor neurons in the larval zebrafish brain[35]. Similarly to the case of 2D-CGH, illumination of spatially closed targets quickly deteriorates the axial resolution[36]. On the other hand using 3D illumination with TF is a challenge because the axially shifted holographic planes cannot be simultaneously imaged on the TF grating.

As a solution, we demonstrated, in 2016, an optical scheme using two spatial light modulators (SLMs) (Figure 2a) to independently control the lateral shape and position of multiple patterns (SLM1) and their axial position (SLM2)[34] by addressing the SLMs in vertical tiles equaling the number of planes to be illuminated (Figure 2b). This strategy enabled for the first time the generation of temporally focused patterns at axially distinct planes, whose axial selectivity demonstrated by 3D photoconversion of multiple targets in the zebrafish larva spinal cord and brain[34]. The main drawback related to the vertical tiling of the SLMs, is that for a number of pixels in the vertical direction (orthogonal to the dispersion direction) ≤ 100[34] the lateral resolution starts deteriorating thus limiting the maximum number of achievable planes to ≈ $N_{SLM}/100$, with N_{SLM} the total number of pixels in the SLM vertical direction (i.e to 6 to 12 planes for mostly commonly used LCOS devices). This limitation can be overcome by using the second SLM for both lateral and axial beam multiplexing as illustrated in Figure 2c[37]. This scheme enables multiplexed temporal focusing light shaping (MTF-LS) with several advantages: firstly, because each spot is the exact replica of what the first SLM generates at the TF grating, the spot quality in the 3D volume is independent on the number of generated planes and axial position. Secondly, MTF-LS is compatible with different light shaping approaches, including dynamic CGH[37], GPC[37–39], CGH with a fixed phase mask[37] and low-NA Gaussian beams[40,41]. Dynamic CGH, has maximal flexibility and enables fast lateral shaping. Replacing the bulky SLM with a smaller static phase mask reduces the flexibility of the system but leads to a simpler and more compact optical design. GPC on the other hand permits generation of illumination patterns with superior axial resolution and higher uniformity (speckle-free) (Figure 2d), which is particularly advantageous for applications requiring spot sizes comparable to the speckle size or for multisite functional imaging. For conventional GPC, the conditions to achieve maximum interferometric contrast impose some restrictions to the optimal spot size and excitation field[17], moreover intensity light shaping is only limited to a single plane (conjugated to the SLM plane; Figure 1b). However, when GPC is implemented

in a MTF-GPC scheme, these limitations can be all overcome: the GPC setup can be designed to generate a shape with optimal diffraction efficiency, multiplexed laterally and axially by the second SLM, thus enabling 3D spot generation within the same excitation field reached in CGH[37–39].

The MTF-LS approach can be further simplified by replacing the first light shaping module with an expanded Gaussian beam, as independently demonstrated by the two groups of M. Booth[40] and H. Adesnik[41]. However, as for MTF-GPC, the use of low-NA Gaussian beams limits the beam size on the SLM in the un-chirped direction to few millimeters[40] thus limiting the maximum power that can be used and therefore the maximum number of achievable targets. Introducing a curvature on the incident Gaussian beam, as proposed by Pégard and colleagues[41], enabled covering the entire SLM and generating hundreds of spots in a 400×400×400 μm^3 excitation volume. However, this solution inevitably separates the spatial from the temporal focal plane and leaves a secondary spatial focus, which deteriorates the axial resolution (Figure 2d). Moreover, the use of a low-NA Gaussian beam is limited to the generation of a non-reconfigurable and single-size spot.

Design of complex, multi-target experiments requires taking into account possible sources of photo-damage to set the maximum number of achievable targets. This includes both thermal damage related to the linear absorption of light, and nonlinear photochemical and ablation damage[42–44]. Scanning approaches require higher intensity but lower average power, so they will be mostly limited by nonlinear damages. Parallel illumination approaches use very low intensity but higher total average power, so they will be mostly limited by thermal damages.

Laser development

Reliable AP generation can be achieved by using conventional femtosecond Ti:Sapphire laser oscillators, commonly adopted in 2P microscopy. However, at the wavelength typically used for photostimulation (i.e. 900–950 nm, Figure 3a) these sources can provide only few Watts output (~200 mW after the objective) which, considering that in vitro AP generation (at depth ≈40 μm), using parallel illumination with these laser sources requires 10–40 mW per cell[45,46], limits the maximum number of simultaneously achievable targets to few cells (<10). Combining these sources with multi-target spiral scanning illumination through CGH can increase this number.

Amplified low repetition rate fiber lasers enable higher 2P absorption compared to Ti:Sapphire oscillators (the 2P excited signal S_{2PE} being proportional to the peak power $P_{avg}/(f\tau)$; with f and τ being the repetition rate[47] and pulse duration, respectively) and therefore reduced spiking power threshold (1–10 mW per cell at depth of ≈40 μm, *in vitro*[45,46]). This, in addition to the capability for these sources to deliver tens of Watts of exit power, makes in principle possible to simultaneously photostimulate hundreds of cells both using parallel and scanning approaches, providing that photodamage thresholds are not reached. Laser sources at the standard repetition rate for oscillators (tens of MHz) can also be used[8] although for multi-cell stimulation one should consider the use of even higher average power. Currently low-repetition rate amplifiers are based on Yb^{3+}-doped fibers and have an emission wavelength in the range of 1030–1060 nm. Development of tunable low-

repetition rate sources will enable to broaden even further the accessible combination of reporters and actuators.

Opsin engineering

Today an ever growing list of optogenetic actuators with different photocycle kinetics, action spectra, light sensitivity and ion conductance (Figure 3a–b)[5,48–50] makes it difficult to choose the optimal optogenetic tool for brain circuits investigation. In the following we will review the criteria that need to be considered when designing an optogenetic experiment with a defined temporal and spatial resolution and/or an "all optical" experiment.

Temporal resolution and kinetics parameters

Opsin-expressing neurons illuminated by a long light pulse show a typical photocurrent trace where one can distinguish a rising, a desensitization and a decay phase (Figure 3a). Each of these phases can be associated to an empirical time constant τ_{on} τ_{inact} and τ_{off} (using a mono-exponential fit), respectively. This set of 'kinetics parameters' together with the values of the peak current and the current plateau can be used as guidance to model the dynamic of photocurrent. The fitting models can have different level of complexity using a three-state[1,51], a four-state[1,51–53] or a six-state model[54] (Figure 3c). The three-state model describes the opsin photocycle using a closed/ground-, an opened- and a closed/desensitized-state, it can qualitatively reproduce the overall kinetics of currents and the peak to plateau ratio as well as admits an analytical solution. The simplicity of the model does not permit, however to account for the bi-exponential off-kinetics of ChR2-mediated photocurrents, and the dark recovery of the peak current. These effects can be well modeled by using a four-state model, which assumes two closed and two open states with different conductivities and lifetimes[1,52]. To date, all these models have been applied to model the electrophysiological reaction schemes of ChR1 and ChR2. For other opsins, the kinetics parameters (τ_{on} τ_{inact} and τ_{off}) have been deduced using a mono-exponential fit of photoevoked currents under 1P-wide-field or 2P-soma-targeted illumination of CHO, HEK cells or neuronal cultures. Overall τ_{on} and τ_{inact} have a non-linear dependence on light irradiance and depend on the excitation wavelength, while τ_{off} can be considered independent of light irradiance. Notably, the kinetics parameters can largely differ from one opsin to another (Figure 3b)[36,46,50,55]. Fast opsins, such as Chronos, have τ_{on} (at saturation) ≈1–2 ms and τ_{off} ≈ 4 ms[36,50,55], while slow opsins, such as ReaChR or $C1V1_{TT}$ have τ_{on} ≈ 6–8 ms (at saturation) and τ_{off} ≈ 50–100 ms[45,50,56]. CoChR and ChrimsonR have intermediate values: τ_{on} ≈ 2–6 ms, τ_{off} ≈ 30 ms[46,50], and τ_{on} ≈ 8 ms, τ_{off} ≈ 15 ms[50], respectively. Notably when comparing the numbers reported in the literature, one needs to take into account possible differences in experimental configurations and data analysis: holographic targeted light on the cell soma gives shorter τ_{off} values with respect to wide-field illumination[46], in cultured cells both τ_{on} and τ_{off} can be slowed down by the presence of gap junctions[57], τ_{on} can be defined either as the time to reach 90% or 1/e of the peak current.

In general, scanning approaches are more suitable with slow opsins (C1V1, ReaChR, CoChR) while parallel approaches can be combined both with slow and fast opsins. Importantly, the efficient current integration under parallel illumination enables to control

neuronal spiking *in vitro*[45,46,55] and *in vivo*[58] with millisecond peak latencies and sub-millisecond jitter (i.e. the standard deviation of latencies) independently of the on-kinetics of the opsin (Figure 3d). The off-kinetics, on the other side affects the maximum achievable spiking rate: for example in vitro 2P holographic illumination targeted on the soma of neurons expressing the slower opsin ReaChR could generate APs at a max spiking rate of 20 Hz or 40 Hz, in slow and fast spiking cells, respectively[25,45,55], while combined with the fast opsin Chronos could generate spiking train of up to 100 Hz with < 1 ms jitter[55]. So far, scanning approaches combined with the opsin C1V1 have been able to produce *in vitro* or *in vivo* reliable spiking trains at maximum frequency of 20 Hz[6].

Single cell resolution and molecular focusing

Although using 2P excitation combined with spiral or spatio-temporally focused beam, enables reducing the illumination volume down to the size of a single cell, still reaching a true cellular resolution is challenged by the expression of the opsin on axons and dendrites. Excitation spots even located several micrometers away from the cell soma can generate high photocurrents[21,59] and voltage spikes[36,45,46] on the targeted cell thus strongly deteriorating the effective spatial resolution.

Several solutions have been proposed to confine the opsin to specific subcellular compartments (see Rost et al. for a detailed review[60]) and recently have been combined with 2P parallel illumination to reach the first demonstrations of optical control of neuronal activity with single-cell resolution in cortical slices[21,46]. In a pioneering work, Baker et al.[21] used a ChR2 fusion proteins by attaching a 65 amino acid motif from the Kv2.1 voltage-gated potassium channel to the carboxy (C) terminus of ChR2-EYFP to target ChR2 to the soma and proximal dendrites of neurons in the mouse somatosensory cortex. With this approach combined with Ca^{2+} imaging they also demonstrated *in vitro* functional connectivity mapping. More recently, Shemesh and colleagues[46] fused the N terminal of the KA2(1–150) (the 150 amino acids of a 360 amino acids fragment of KA2) to the C terminus of GFP-CoChR to achieve somatic expression of CoChR, whose high efficiency enabled to trigger AP with <1 ms jitter and <15 ms latency in mouse cortical brain slices. Combined with multi-site holographic stimulation and low repetition fiber lasers the use of soCoChR also enabled 3D multi targeted activation with reduced cross talk (Figure 4) and perform connectivity experiment with electrophysiological detection of post synaptic responses with millisecond precision.

All optical brain recording

Knowing opsin action spectra and kinetics parameters is crucial when designing multi-wavelength experiments that aim at independently activate a specific combination of actuator and reporter. Although the 2P action spectra peak of most commonly used opsins spans from blue (880 nm) to red (> 1100 nm) (Figure 3a), they are all very broad (FWHM ≈ 50 nm) with a blue tail extending for tens of nanometers. Therefore practically every opsin has non-zero absorption at the wavelength typically used for GCaMP 2P-imaging (920–950 nm), with consequent artefactual opsin activation by the imaging laser.

Different solutions have been proposed to minimize this cross talk, although none of these approaches have so far proved true zero artifactual depolarization during imaging. This includes 2P parallel illumination with somatic opsin (ChR2-P2A-H2B-mRuby2; photostimulation at 880 nm) combined with GCaMP6s 2P imaging (920 nm)[21], 2P scanning photostimulation of C1V1-2A-mCherry (1064 nm) combined with fast (30 Hz, scaning rate) GCaMP6s imaging (920 nm)[8], 2P holographic photostimulation (920 nm) of ChR2-mCherry combined with nuclear-localized GCaMP6s imaging at 1020 nm[35] or 2P holographic photostimulation (1030 nm) of ReachR-dTomato combined with low power GCaMP6s imaging[58]. Using fast and red shifted opsins, as ChrimsonR, combined with green shifted activity reporter, or blue shifted opsins combined with red Ca^{2+} indicators should enable to minimize the cross talk even further. For investigation of connectivity among independent neuronal population a convenient solution could be to use non overlapping expression of actuators and sensors[61].

Outlook

Until now, the typical peak power values used for excitation with parallel illumination seem to be below the threshold for ablation damage[42] they however may fall well in the range of thermal damage for prolonged exposure time[42]. Design of complex, multi-target experiments will require careful modeling of light spreading and heat dissipation to find the conditions (pulse duration, average target separation and stimulation frequency) that minimize temperature rise. Until now 2P optogenetics have been demonstrated at depths of 250–300 μm[9,24]. Optical manipulation of deeper circuits will require the combination of patterned light illumination with endoscopic probes (e.g. GRIN lens)[62], eventually combined with flexible fiber bundles[63], or three-photon excitation[64,65]. All-optical circuit manipulation on large volumes, near the mm^3 range, will require clever combinations for simultaneous multi-target activation and concurrent activity reading (see also review by W. Yang and R. Yuste on this same issue). Engineering of SLMs with more pixels will enable increasing even further the accessible field of excitation. Development of fast and more sensitive opsins will enable to further reduce the illumination time and therefore the achievable temporal resolution and precision.

Overall “circuit optogenetics” requires joint progress in multi-disciplines such as molecular biology, optics, modeling, biophysics, opsin engineering, and neurophysiology. The knowledge in each respective field can be very far apart and hardly embraced by a single scientist. The success of “circuit optogenetics” depends therefore, and more than ever, on a committed joint effort to deliver and disseminate trustworthy technology.

Acknowledgments

We thank Marta Gajowa, Alexis Picot and Dimitrii Tanese for the unpublished data presented in Figure 3(a)(ii).

IWC received funding from the European Union’s Horizon 2020 research and innovation program under the Marie Skłodowska-Curie grant agreement no. 747598. EP acknowledges the ‘Agence Nationale de la Recherche’ ANR (3DHoloPAc), VE acknowledges the Human Frontiers Science Program (Grant RGP0015/2016), the National Institutes of Health (Grant NIH U01NS090501-03) and the Getty lab. This research was also developed with funding from the Defense Advanced Research Projects Agency (DARPA), contract No. N66001-17-C-4015. The views, opinions and/or findings expressed are those of the author and should not be interpreted as representing the official views or policies of the Department of Defense or the US Government.

References

Papers of particular interest, published within the period of review, have been highlighted as:

* of special interest

** of outstanding interest

1. Nagel G, et al. Channelrhodopsin-2, a directly light-gated cation-selective membrane channel. Proc Natl Acad Sci U S A. 2003; 100:13940–13945. [PubMed: 14615590]
2. Boyden ES, Zhang F, Bamberg E, Nagel G, Deisseroth K. Millisecond-timescale, genetically targeted optical control of neural activity. Nat Neurosci. 2005; 8:1263–1268. [PubMed: 16116447]
3. Boyden ES. Optogenetics and the future of neuroscience. Nat Neurosci. 2015; 18:1200–1201. [PubMed: 26308980]

4**. Rickgauer JP, Tank DW. Two-photon excitation of channelrhodopsin-2 at saturation. Proc Natl Acad Sci U S A. 2009; 106:15025–15030. First demonstration of action potential generation in cultured neurons using 2P laser scanning and optogenetics. [PubMed: 19706471]

5. Yizhar O, et al. Neocortical excitation/inhibition balance in information processing and social dysfunction. Nature. 2011; 477:171–178. [PubMed: 21796121]

6**. Prakash R, et al. Two-photon optogenetic toolbox for fast inhibition, excitation and bistable modulation. Nat Methods. 2012; 9:1171–9. First demonstration of action potential generation in vivo using 2P laser scanning and optogenetics. [PubMed: 23169303]

7. Packer AM, et al. Two-photon optogenetics of dendritic spines and neural circuits. Nat Methods. 2012; 9:1171–1179. [PubMed: 23169303]

8**. Packer AM, Russell LE, Dalgleish HWP, Häusser M. Simultaneous all-optical manipulation and recording of neural circuit activity with cellular resolution in vivo. Nat Methods. 2015; 12:140–146. First demonstration of in vivo 2P all-optical circuit manipulation combining spiral scanning of multiple holographic spots and Ca^{2+} imaging. [PubMed: 25532138]

9*. Yang W, Carrillo-reid L, Bando Y, Peterka DS, Yuste R. Simultaneous Two-photon Optogenetics and Imaging of Cortical Circuits in Three Dimensions. eLife. 2018; 7:e32671. A recent study demonstrating 3D all-optical investigation *in vivo* by using the hybrid illumination method for optogenetic activation. [PubMed: 29412138]

10. Curtis JE, Koss BA, Grier DG. Dynamic holographic optical tweezers. Opt Commun. 2002; 207:169–175.
11. Glückstad J. Phase contrast image synthesis. Opt Commun. 1996; 130:225–230.

12**. Lutz C, et al. Holographic photolysis of caged neurotransmitters. Nat Methods. 2008; 5:821–827. First demonstration of holographic light shaping for neuronal activation using 1P glutamate uncaging in brain slices. [PubMed: 19160517]

13*. Papagiakoumou E, de Sars V, Oron D, Emiliani V. Patterned two-photon illumination by spatiotemporal shaping of ultrashort pulses. Opt Express. 2008; 16:22039–22047. First demonstration of temporally-focused arbitrary light shaping, by combining phase modulation of light with temporal focusing. [PubMed: 19104638]

14. Oron D, Tal E, Silberberg Y. Scanningless depth-resolved microscopy. Opt Express. 2005; 13:1468–1476. [PubMed: 19495022]
15. Zhu G, van Howe J, Durst M, Zipfel W, Xu C. Simultaneous spatial and temporal focusing of femtosecond pulses. Opt Express. 2005; 13:2153–2159. [PubMed: 19495103]
16. Papagiakoumou E, de Sars V, Emiliani V, Oron D. Temporal focusing with spatially modulated excitation. Opt Express. 2009; 17:5391–5401. [PubMed: 19333304]

17**. Papagiakoumou E, et al. Scanless two-photon excitation of channelrhodopsin-2. Nat Methods. 2010; 7:848–854. First demonstration of parallel activation of a single and multiple neurons in brain slices using GPC and temporal focusing. [PubMed: 20852649]

18. Bègue A, et al. Two-photon excitation in scattering media by spatiotemporally shaped beams and their application in optogenetic stimulation. Biomed Opt Express. 2013; 4:2869–2879. [PubMed: 24409387]

19. Andrasfalvy BK, Zemelman BV, Tang J, Vaziri A. Two-photon single-cell optogenetic control of neuronal activity by sculpted light. Proc Natl Acad Sci U S A. 2010; 107:11981–11986. [PubMed: 20543137]

20. Rickgauer JP, Deisseroth K, Tank DW. Simultaneous cellular-resolution optical perturbation and imaging of place cell firing fields. Nat Neurosci. 2014; 17:1816–1824. [PubMed: 25402854]

21**. Baker CA, Elyada YM, Parra-Martin A, Bolton M. Cellular resolution circuit mapping in mouse brain with temporal-focused excitation of soma-targeted channelrhodopsin. eLife. 2016; 5:1–15. First demonstration of in vitro soma-localized activity using somatic-C1V1 and a temporally focused Gaussian beam.

22. Straub C, et al. Principles of Synaptic Organization of GABAergic Interneurons in the Striatum. Neuron. 2016; 92:84–92. [PubMed: 27710792]

23. Sela G, Dana H, Shoham S. Ultra-deep penetration of temporally-focused two-photon excitation. 2013; 8588:10–15.

24. Papagiakoumou E, et al. Functional patterned multiphoton excitation deep inside scattering tissue. Nat Photonics. 2013; 7:274–278.

25*. Ronzitti E, et al. Recent advances in patterned photostimulation for optogenetics. J Opt. 2017; 19:113001. A recent detailed overview on photoactivation methods used so far for optogenetics.

26. Leach J, et al. Interactive approach to optical tweezers control. Appl Opt. 2006; 45:897–903. [PubMed: 16512531]

27*. Nikolenko V, et al. SLM Microscopy: Scanless Two-Photon Imaging and Photostimulation with Spatial Light Modulators. Front Neural Circuits. 2008; 2:5. First demonstration of 2P-CGH for multi site uncaging. [PubMed: 19129923]

28. Yang S, et al. Three-dimensional holographic photostimulation of the dendritic arbor. J Neural Eng. 2011; 8:46002.

29**. Anselmi F, et al. Three-dimensional imaging and photostimulation by remote-focusing and holographic light patterning. Proc Natl Acad Sci U S A. 2011; 108:19504–19509. First demonstration of all-optical manipulation of neuronal activity by using 3D multi-site holographic uncaging and 3D Ca^{2+} imaging using remote focusing. [PubMed: 22074779]

30. Daria VR, Stricker C, Bowman R, Redman S, Bachor HA. Arbitrary multisite two-photon excitation in four dimensions. Appl Phys Lett. 2009; 95:93701.

31. Gerchberg RW, Saxton WO. A pratical algorithm for the determination of the phase from image and diffraction pictures. Optik (Stuttg). 1972; 35:237–246.

32. Piestun R, Spektor B, Shamir J. Wave fields in three dimensions: analysis and synthesis. J Opt Soc Am A. 1996; 13:1837.

33. Haist T, Schönleber M, Tiziani H. Computer-generated holograms from 3D-objects written on twisted-nematic liquid crystal displays. Opt Commun. 1997; 140:299–308.

34**. Hernandez O, et al. Three-dimensional spatiotemporal focusing of holographic patterns. Nat Commun. 2016; 7:11928. First demonstration of generation of multiple temporally-focused shapes at axially distinct planes by decoupling the lateral from the axial wavefront shaping. [PubMed: 27306044]

35*. dal Maschio M, Donovan JC, Helmbrecht TO, Baier H. Linking Neurons to Network Function and Behavior by Two-Photon Holographic Optogenetics and Volumetric Imaging. Neuron. 2017; 94:774–789.e5. First demonstration of all-optical neuronal circuits manipulation using 2P 3D-CGH and 2P Ca^{2+} imaging in the zebrafish larvae. [PubMed: 28521132]

36. Papagiakoumou, E., et al. Two-Photon Optogenetics by Computer-Generated Holography. In: Stroh, A., editor. Optogenetics: A roadmap, Neuromethods. Vol. 133. Humana Press; New York: 2018. p. 175-197.

37*. Accanto N, et al. Multiplexed temporally focused light shaping for high-resolution multi-cell targeting. bioRxiv. 2017 First demonstration of volumetric multiplexing of temporally-focused shapes generated with static and dynamic CGH, or GPC.

38. Go MA, Ng P-F, Bachor Ha, Daria VR. Optimal complex field holographic projection. Opt Lett. 2011; 36:3073–5. [PubMed: 21847164]

39*. Bañas A, Glückstad J. Holo-GPC: Holographic Generalized Phase Contrast. Opt Commun. 2017; 392:190–195. First demonstration of Holo-GPC, enabling to create 3D replicas of a GPC spot *via* CGH.

40*. Sun, B., et al. Four-dimensional light shaping: manipulating ultrafast spatio-temporal foci in space and time; arXiv. 2017. p. 1-14.at <http://arxiv.org/abs/1705.05433> First demonstration of lateral and axial multiplexing of a low-NA temporally-focused Gaussian beam *via* CGH

41*. Pegard NM, Oldenburg I, Sridharan S, Wallller L, Adesnik H. 3D scanless holographic optogenetics with temporal focusing. Nat Commun. 2017; 8:1228. First demonstration of 3D volumetric projection of hundreds of low-NA temporally focused Gaussian beams *via* CGH. [PubMed: 29089483]

42. Boulnois JL. Photophysical processes in recent medical laser developments: A review. Lasers Med Sci. 1986; 1:47–66.

43. Koester HJ, Baur D, Uhl R, Hell SW. Ca2+ fluorescence imaging with pico- and femtosecond two-photon excitation: signal and photodamage. Biophys J. 1999; 77:2226–2236. [PubMed: 10512842]

44. Hopt, a, Neher, E. Highly nonlinear photodamage in two-photon fluorescence microscopy. Biophys J. 2001; 80:2029–36. [PubMed: 11259316]

45*. Chaigneau E, et al. Two-photon holographic stimulation of ReaChR. Front Cell Neurosci. 10:234–2016. First demonstration of in vitro 2P activation of the opsin ReaChR and of 2P optogenetics activation using a low-repetition rate fiber laser.

46**. Shemesh OA, et al. Temporally precise single-cell resolution optogenetics. Nat Neurosci. 2017; 20:1796–1806. First demonstration of in vitro optical control of spiking activity of a single and multiple neurons with sub-millisecond jitter and single cell resolution using somatic-CoChR and temporally-focused CGH. [PubMed: 29184208]

47. Denk W, Strickler JH, Webb WW. Two-photon laser scanning fluorescence microscopy. Science. 1990; 248:73–76. [PubMed: 2321027]

48. Schneider F, Grimm C, Hegemann P. Biophysics of Channelrhodopsin. Annu Rev Biophys. 2015; 44:167–186. [PubMed: 26098512]

49. Mattis J, et al. Principles for applying optogenetic tools derived from direct comparative analysis of microbial opsins. Nat Methods. 2011; 9:159–172. [PubMed: 22179551]

50*. Klapoetke NC, et al. Independent optical excitation of distinct neural populations. Nat Methods. 2014; 11:338–346. First demonstration and characterization of several efficient variants of ChR such as Chronos, CoChR, Chrimson using 1P wide-field illumination. [PubMed: 24509633]

51. Nikolic, K., Degenaar, P., Toumazou, C. Modeling and engineering aspects of ChannelRhodopsin2 system for neural photostimulation. Annual International Conference of the IEEE Engineering in Medicine and Biology - Proceedings; 2006. p. 1626-1629.

52. Hegemann P, Ehlenbeck S, Gradmann D. Multiple photocycles of channelrhodopsin. Biophys J. 2005; 89:3911–8. [PubMed: 16169986]

53. Nikolic K, et al. Photocycles of Channelrhodopsin-2. Photochem Photobiol. 2009; 85:400–411. [PubMed: 19161406]

54. Grossman N, et al. The spatial pattern of light determines the kinetics and modulates backpropagation of optogenetic action potentials. J Comput Neurosci. 2012; 2

55*. Ronzitti E, et al. Sub-millisecond optogenetic control of neuronal firing with two-photon holographic photoactivation of Chronos. J Neurosci. 2017; 37:10679–10689. First demonstration of in vitro 2P activation of the opsin Chronos and CoChR, and first demonstration of optically induced fast spiking (100 Hz) train activation using 2P illumination. [PubMed: 28972125]

56*. Lin JY, Knutsen PM, Muller A, Kleinfeld D, Tsien RY. ReaChR: a red-shifted variant of channelrhodopsin enables deep transcranial optogenetic excitation. Nat Neurosci. 2013; 16:1499–1508. First demonstration and characterization of the opsin ReaChR using 1P wide field illumination. [PubMed: 23995068]

57. Conti R, Assayag O, De Sars V, Guillon M, Emiliani V. Computer generated holography with intensity-graded patterns. Front Cell Neurosci. 2016; 10:236. [PubMed: 27799896]

58**. Chen I-W, et al. Parallel holographic illumination enables sub-millisecond two-photon optogenetic activation in mouse visual cortex in vivo. bioRxiv. 2017; :1–21. First demonstration of optical control of neuronal activity in vivo with millisecond latency and sub-millisecond jitter

using CGH and temporal focusing for opsins with different channel kinetics. DOI: 10.1101/250795

59. Madisen L, et al. A toolbox of Cre-dependent optogenetic transgenic mice for light-induced activation and silencing. Nat Neurosci. 15:793–802.
60. Rost BR, Schneider-Warme F, Schmitz D, Hegemann P. Optogenetic Tools for Subcellular Applications in Neuroscience. Neuron. 2017; 96:572–603. [PubMed: 29096074]
61. Förster D, Maschio MD, Laurell E, Baier H. An optogenetic toolbox for unbiased discovery of functionally connected cells in neural circuits. Nat Commun. 2017; 8:116. [PubMed: 28740141]
62. Moretti C, Antonini A, Bovetti S, Liberale C, Fellin T. Scanless functional imaging of hippocampal networks using patterned two-photon illumination through GRIN lenses. Biomed Opt Express. 2016; 7:3958. [PubMed: 27867707]
63. Szabo V, Ventalon C, De Sars V, Bradley J, Emiliani V. Spatially Selective Holographic Photoactivation and Functional Fluorescence Imaging in Freely Behaving Mice with a Fiberscope. Neuron. 2014; 84:1157–1169. [PubMed: 25433638]
64. Horton NG, et al. In vivo three-photon microscopy of subcortical structures within an intact mouse brain. Nat photonics. 2013; 7:205–209.
65. Rowlands CJ, et al. Wide-field three-photon excitation in biological samples. Light Sci Appl. 2016; 6:e16255.
66. Chen TW, et al. Ultrasensitive fluorescent proteins for imaging neuronal activity. Nature. 2013; 499:295–300. [PubMed: 23868258]
67. Dana H, et al. Sensitive red protein calcium indicators for imaging neural activity. eLife. 2016; 5:1–24.

Highlights

- Manipulation of brain circuits requires millisecond precision and single-cell resolution
- Two-photon optogenetics enable neuronal manipulation in depth
- Wavefront shaping enables resolved 3D multi-target illumination
- Parallel illumination enables control of neuronal activity with millisecond resolution
- Soma-targeted opsins enable control of neuronal activity with single-cell precision

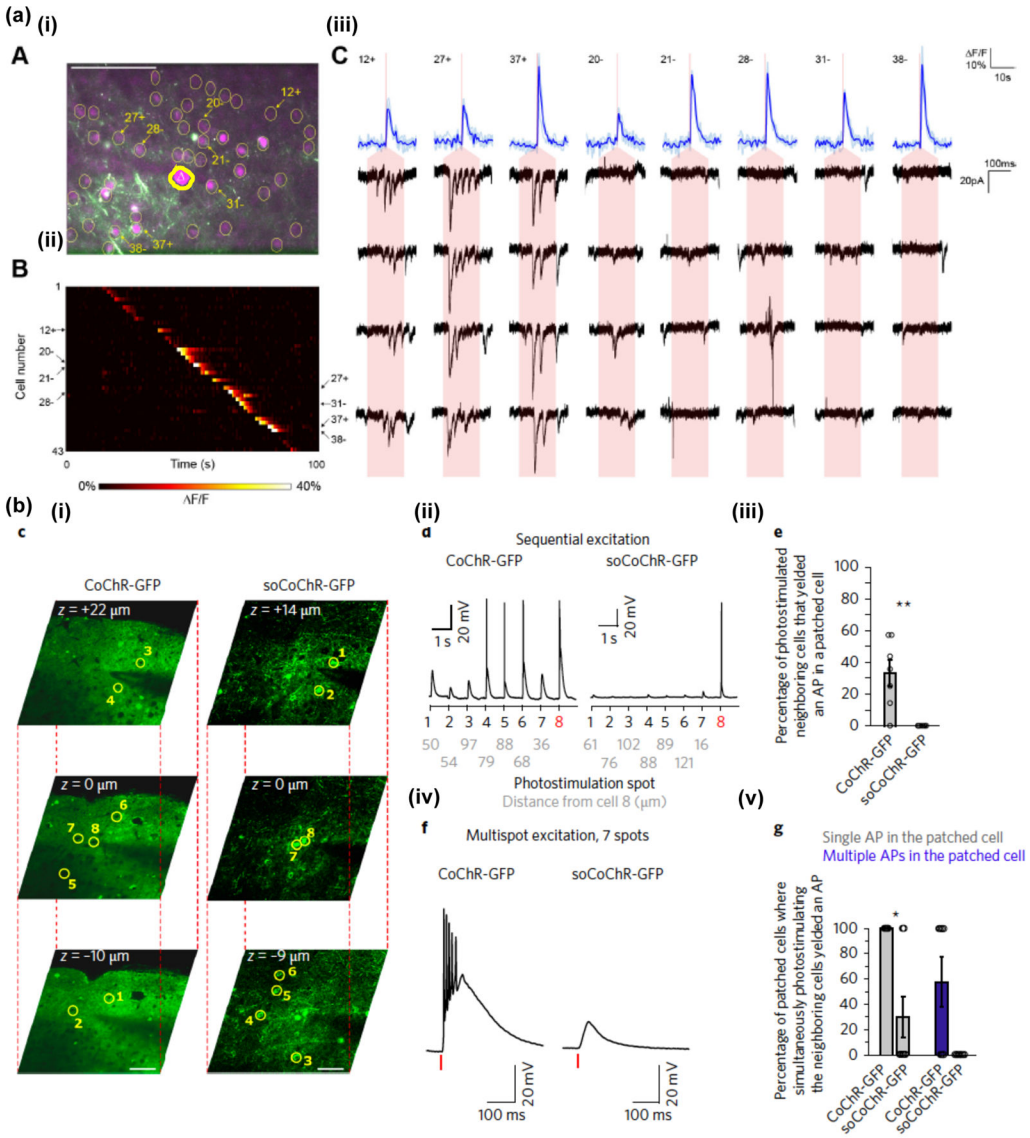

Figure 1. Spatiotemporal light-shaping

(a) Experimental scheme for microscope-implementation of Computer-Generated Holography (CGH). A laser beam is expanded (lenses L1, L2) to fit the SLM array size. The SLM is then imaged through lenses L3, L4 at the back focal plane (BFP) of the microscope objective (OBJ), and thus conjugated to the BFP (BFP*). Arbitrary intensity patterns are projected at the objective front focal plane (FFP) by phase modulation of the illumination beam at its BFP by means of the SLM. A user-defined pattern, usually based on a fluorescence image of the sample, is transformed to a binary image used as the input for the iterative-Fourier transform based algorithm (inset, left). The output of the algorithm is then a gray-scale image where each gray level is associated to a phase delay φ_i ranging from 0 to 2π (inset, middle), and this consists the phase profile addressed to the SLM; a speckled holographic-based intensity distribution is generated at the FFP (here visualized by two-photon excitation of a thin fluorescent layer (inset, right). (b) Experimental scheme for microscope-implementation of Generalized Phase Contrast (GPC). Here, the SLM is

conjugated to the objective FFP (FFP*) through lenses L3, L4, L5 and the OBJ. Arbitrary intensity patterns are obtained by generating a binary input image again (inset, left), which is directly transformed to a binary (0, π) phase profile (inset, left) and addressed to the SLM. A Phase Contrast Filter (PCF) placed in a BFP* plane, introduces a π-phase shift between low- and high-spatial frequencies (highlighted, respectively, as red and light red in the figure) of the focused light, after being diffracted by the SLM. The binary image of the user-defined pattern is in this case transformed to a phase image encoded for 0/π phase shifts and it is addressed to the SLM (inset middle). The output of the GPC method is then a uniform intensity distribution corresponding exactly to the phase pattern addressed to the SLM, generated at the focal plane of lens L4, which is conjugate to the objective FFP through L5 and the OBJ. (c) Temporal focusing of ultrashort pulses. In the spectral representation shown here temporal focusing can be interpreted by the in-phase recombination at the objective focal plane of the spectral frequencies comprising the ultrashort pulses of the input laser beam (beam incident onto the grating at an angle α), after their dispersion on the diffraction grating. Images adapted from Ronzitti et al.[25]

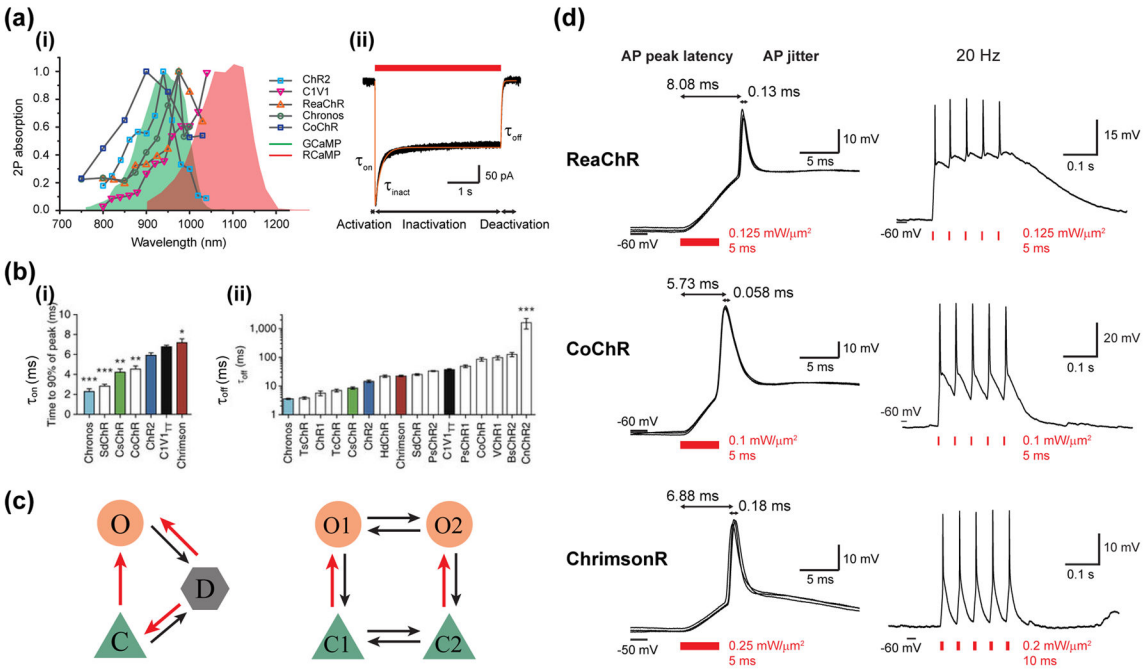

Figure 2. Multiplane temporally focused pattern projection

(a) Experimental scheme for multi-plane temporally focused patterns. The system comprises a first beam-shaping part, which, according to the experimental needs, can generate a Gaussian, a holographic or a GPC beam. Here, the case of a CGH beam is shown (red dashed box). The second part performs temporal focusing (TF) through the diffraction grating G, L2 and L3, and spatial beam multiplexing through SLM2 and L3 *via* CGH (blue dashed box). L4 and OBJ rescale the 3D pattern configuration at the sample volume. (b, c) Examples of different ways for addressing the two SLMs in the scheme presented in (a) for MTF-CGH: (b) (i) SLM1 is vertically tiled in different areas, each area addressed with independent phase profiles, which in the present paradigm project the words ‘neuro’ and ‘photonics’ in two different planes A and B. (ii) SLM2 is addressed with two Fresnel lens-phase profiles to axially displace each holographic pattern generated by SLM1 on separate planes, in this case at +20 μm (plane A) and −20 μm (plane B). (iii) Phase profile resulting at the objective back focal plane for a single spectral frequency. (iv) Intensity distribution at the focal plane of the objective. Adapted from Hernandez et al.[34]. (c) Multiplexed temporally-focused CGH. (i) In this case, SLM1 is addressed with a phase hologram encoding the desired excitation pattern, e.g. a star. (ii) SLM2 is addressed with a phase profile encoding a 3D-diffraction-limited spots distribution. (iii) Resulting phase profile at the objective back focal plane creating multiple replicas of the pattern generated by the first SLM. (iv) Application of the method for projecting 50 15-μm diameter circular temporally focused spots in a volume of 300×300×500 μm^3. Adapted from Accanto et al.[37] (d) Illustration of different beam shaping methods that could be used in MTF-LS configurations. The *x-y*, *y-z* cross-sections and axial intensity profiles along the yellow dashed lines of the *y-z* cross-sections are shown for (i) MTF-CGH, (ii) MTF-GPC, and (iii) large Gaussian beams (3D-SHOT). In the latter case both experimental data and simulation are shown. Green arrow

indicates the primary focus of the method and magenta arrow indicates the secondary focus. Adapted from Pégard et al.[41].

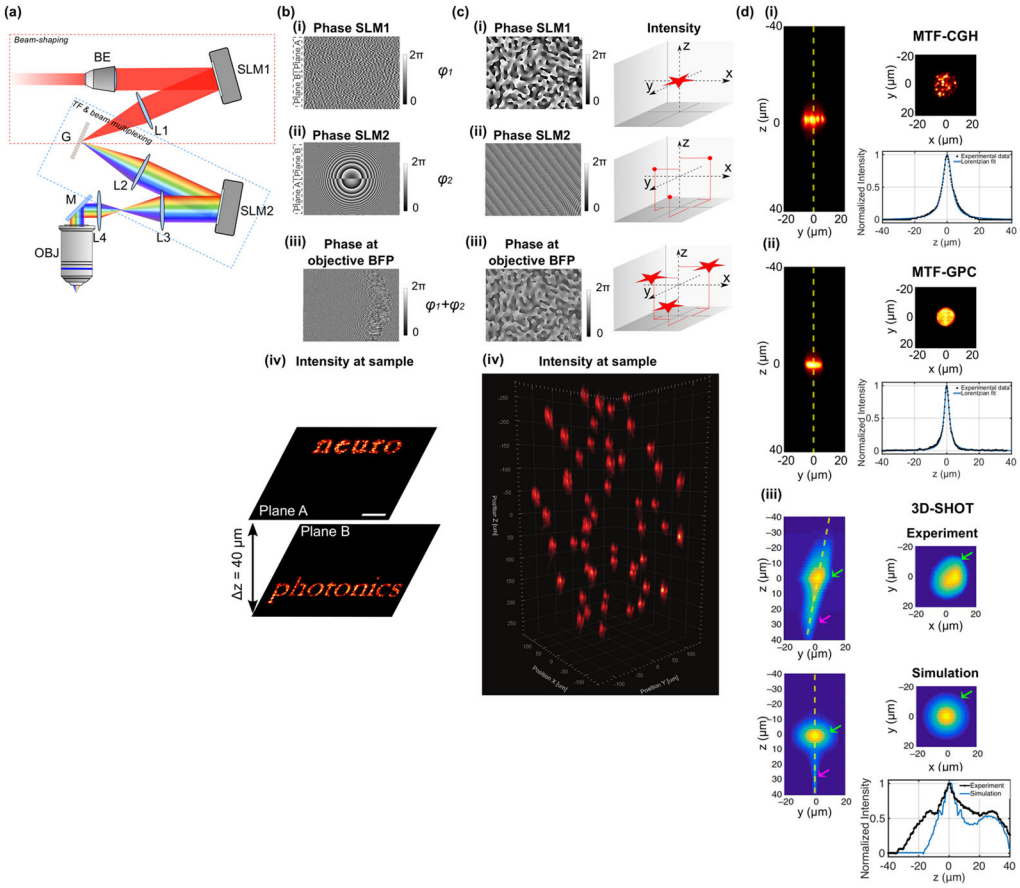

Figure 3. Optogenetic toolbox and two-photon holographic activation

(a) 2P activation of optogenetic actuators. (i) 2P action spectra of diverse opsins[6,45,46,55] (grey lines with coloured markers) overlayed to the absorption spectrum of GCaMP[66] and RCaMP[67]. (ii) Representative trace of photocurrent in a CoChR-expressing Chinese Hamster Ovary (CHO) cell evoked by a 4-s illumination of 0.7 mW/μm^2 at 920 nm through a 15-μm diameter holographic spot (black line). The experimental data is reproduced by a simulation trace (orange line) based on the three-state model (see below). (b) On-kinetics (i) and off-kinetics (ii) of different opsins upon 1P illumination. Channel open rates τ_{on} are determined as the time to 90% peak photocurrent measured in cultured neuron. Channel closing rates τ_{off} are computed by fitting a monoexponential to the 1-s light-off current (Adapted from Klapoetke et al.[50]). (c) Schematics of common photocycle models. The three-state model (left) involves a closed state (C), an open state (O), and a desensitized state (D), whereas the four-state model (right) engages two open states O1 and O2, which can be transformed from two closed states C1 and C2 respectively. Red arrows indicate photo-sensitive transitions between states. (d) 2P holographic illumination enables fast and temporally precise *in vivo* AP generation for neurons expressing ReaChR, CoChR or ChrimsonR in mouse visual cortex. Left: brief pulse-illumination of low intensity at 1030 nm induces APs of millisecond average peak latency (relative to the illumination onset) and sub-millisecond jitter (standard deviation of latencies) in three exemplary cells. Right: A

train of APs is generated following 5 light-pulses occurring at 20 Hz for the 3 opsins. Adapted from Chen et al.[58].

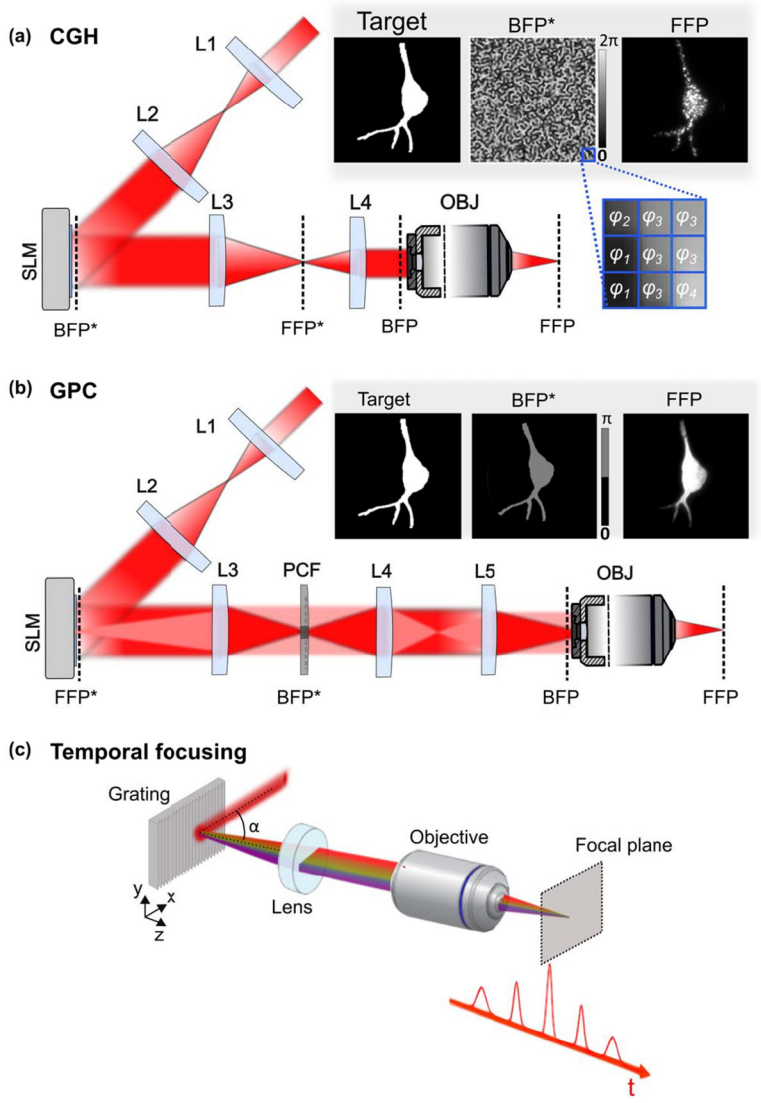

Figure 4. Somatic opsins enable unbiased single-cell photoactivation and identifying neuronal connections

(a) Mapping neuronal connection by co-expressing the calcium indicator GCaMP6s and the somatic ChR2-P2A-H2B-mRubys. (i) In an example field-of-view (FOV) in acute brain slice of layer 2/3 mouse somatosensory cortex, the cytosol expression of mRubys (magenta) induced by the P2A sequence provides clear visualization of individual cells (yellow circles) for photostimulation. Postsynaptic responses are monitored via a patch-pipette (a triangle marker and thicker outline indicates the patched cell). Scale bar 100 μm. (ii) 35 cells in the above FOV display calcium transients upon sequentially scanning a TF laser beam at 880 nm across cell somata. (iii) Postsynaptic activity (4 repetitions shown as black traces) from the patched neuron in response to suprathreshold photoactivation in 8 presynaptic cells (blue traces at the upper raw). 3 cells show postsynaptic responses, thus being connected to the patched cell; the other 5 unconnected cells do not display clear postsynaptic current. Red shades indicate photostimulation epoch of 150 ms. Adapted from Baker et al.[21]. (b) 3D photoactivation with single-cell resolution by using the somatic CoChR. (i) 2P images taken

at 3 z-positions in acute brain slices of layer 2/3 mouse visual cortex which express the non-somatic CoChR-GFP (left) and the somatic CoChR-GFP (right). The patched cells (number 8) and cells nearby (number 1–7) are denoted by yellow circles. Scale bar 50 μm. (ii) Example membrane potential from the patched neuron in response to sequential stimulation of the 7 neighbouring cells with 30-ms TF holographic illumination of 0.1 mW/μm^2 at 1030 nm. Grey numbers indicate the radial distance between the stimulated cell and the patched cell. (iv) Whole-cell recordings of the patched cells while simultaneously stimulating the 7 neurons nearby for CoChR and soCoChR. Red bars indicate photostimulation epochs of the above condition. (iii, v) Compared to non-somatic CoChR, AP generation in the patched neuron is significantly decreased while photostimulating nearby cells, both sequentially and simultaneously, for somatic CoChR, thus ensuring single-cell resolution (n=7 for CoChR and soCoChR; mean±s.e.m.). Adapted from Shemesh et al.[46].